Advanced Composite Materials
Publication details, including instructions for authors and subscription information:
http://www.tandfonline.com/loi/tacm20

Response of composite plates with random material properties using FEM and Monte Carlo simulation

B. Navaneetha Raj [a] , N.G.R. Iyengar [b] & D. Yadav [c]
[a] Department of Aerospace Engineering, I.I.T. Kanpur 208 016, India
[b] Department of Aerospace Engineering, I.I.T. Kanpur 208 016, India
[c] Department of Aerospace Engineering, I.I.T. Kanpur 208 016, India
Version of record first published: 02 Apr 2012.

To cite this article: B. Navaneetha Raj , N.G.R. Iyengar & D. Yadav (1998): Response of composite plates with random material properties using FEM and Monte Carlo simulation, Advanced Composite Materials, 7:3, 219-237

To link to this article: http://dx.doi.org/10.1163/156855198X00165

Adv. Composite Mater., Vol. 7, No. 3, pp. 219–237 (1998)

Response of composite plates with random material properties using FEM and Monte Carlo simulation

B. NAVANEETHA RAJ, N. G. R. IYENGAR and D. YADAV
Department of Aerospace Engineering, I.I.T. Kanpur 208 016, India

Abstract—Composite materials have a large number of parameters associated with their manufacturing. It is not physically possible to control all these parameters, and hence variation in the material properties result. In this paper, for a better modeling of the material properties, these are treated as random variables. Static response characteristics of graphite/epoxy composite laminates are obtained with the help of Monte Carlo simulation and the Finite Element Method (FEM) for different boundary conditions, thickness ratio, aspect ratios and fiber orientations. The input material property mean and variance are assumed to be known. From the limited analytical study conducted it is observed that a single design curve can predict normalized characteristics for all the parameters considered.

Keywords: Composite; laminates; material property; random; deflection.

NOTATION

a	length of the laminate
b	width of the laminate
h	thickness of the laminate
a/h	thickness ratio
AR	aspect ratio
CC	clamped–clamped (plate)
E_l	longitudinal modulus
E_t	transverse modulus
G_{lt}	in-plane shear modulus
G_{tz}, G_{lz}	transverse shear modulii
l, t, z	material axes of the laminate
RV	random variable
SD	standard deviation

SS	simply supported (plate)
U	strain energy
V	potential energy
u, v, w	displacements along x, y and z directions
u_0, v_0, w_0	mid plane displacements
x, y, z	reference axes of the laminate

Greek

μ	mean
ν	Poisson's ratio
σ	standard derivation

1. INTRODUCTION

The mechanical and physical properties of the fiber, resin, etc. constituting the lamina, as provided by the manufacturers, are generally average properties subject to specific production conditions. Because of inherent variations in the production conditions from batch to batch, dispersion in the properties of the raw materials always exists.

The raw materials are combined in a specific proportion to form a lamina. Factors such as temperature, pressure, humidity, fiber spacing, voids, curing time, etc. enter along with the variations in the properties of the raw material. These variations result in the variation of lamina properties. The laminae are stacked together to form laminates and, therefore, variations are present in the stiffness coefficients of the laminates. Tables 1 and 2 show the variations observed in strength and stiffness properties of composite laminates in a moulding lot [1]. These variations in strength and stiffness properties introduce a factor of uncertainty in the response of structures made up of composite materials. Accurate predictions of system behaviour call for a probabilistic analysis approach for composites by modeling their mechanical and physical properties as random variables (*RV*s).

Ibrahim [2] reviewed a number of topics pertaining to structural dynamics with random parameter uncertainties. Nakagiri *et al.* [3] studied simply supported (SS) graphite/epoxy laminates with a Stochastic Finite Element Method (SFEM) taking fiber orientation, thickness of each layer and numbers of layers as random variables and showed that the overall stiffness of the laminate is largely dependent on fiber orientation. Leissa and Martin [4] showed that the variation of fiber spacing or redistribution of fibers tends to increase the buckling load by 38% and fundamental natural frequency by 21% for rectangular composite plates. Englestad and Reddy [5] employed Monte Carlo simulation and different probabilistic distributions to represent the uncertainty of constituent level

Table 1.
Variation of stiffness properties for a widely used graphite/epoxy composite from five sources

Elastic constants (10^6 psi)	1	2	3	4	5	Max. diff. %
Long. tensile modulus	20.8	18.1	21.00	20.6	18.5	16
Long. comp. modulus	18.6	14.5	21.00	19.3	18.5	45
Trans. tensile modulus	1.9	1.8	1.7	1.3	1.6	46
In-plane shear modulus	0.85	—	0.65	0.80	0.65	31
Poisson's ratio	0.30	—	—	0.32	0.25	28

Table 2.
Variation of strength properties for a widely used graphite/epoxy composite from five sources

Strength properties (10^3 psi)	1	2	3	4	5	Max. diff. %
Long. tension	274	190	180	164	169	67
Long. compression	280	126	180	126	162	122
Trans. tension	9.5	5.2	8.0	5.4	6.0	83
Trans. compression	39	—	30	21	25	86
In-plane shear	17.3	—	12	8.4	—	106
Interlaminar shear	—	13.5	13	—	7.1	90

properties in metal matrix composites. Vinckenroy and de Wilde [6] established a procedure to obtain the best fit for each material property to study the behaviour of perforated plates and determine the probability distribution of the response. Salim *et al.* [7–9] studied the statistical response of the composite laminates considering longitudinal modulus $[E_l]$, transverse modulus $[E_t]$, Poisson's ratio $[\nu_{lt}]$ etc. as independent random variables. Salim *et al.* [9] have shown that there is a change in the mode shape with a change in the SD of input *RV*s.

Salim *et al.* [8] employed Rayleigh Ritz formulation along with perturbation technique for the analysis of composite laminates. However, this technique is limited to simple plate geometries and small variations in input variables.

In the present investigation, second order statistics of the basic material properties are assumed to be known. Using Monte Carlo simulation a large sample of material properties are generated to form an ensemble with the given statistical description. The effect of the dispersion in the input material properties of the laminate on the static response of the plate is studied by employing FEM and, using the input ensemble of laminate properties, the response ensemble is obtained. This is analysed to obtain the response statistics.

2. FORMULATION

As stated in the previous section finite element technique is employed for analysing the deflection behaviour of laminates made up of composite material. The laminate is subjected to either uniform loading or sinusoidally varying load.

2.1. Displacement field

Figure 1 shows the rectangular laminated plate considered for the investigation: u, v, w are the displacements along the x, y and z axes, respectively; u_0, v_0 and w_0 represent the mid-plane displacements and ψ_x and ψ_y are the rotations of the normals to the mid-plane after deformation. The displacement field corresponding to the higher order shear deformation theory (HSDT) proposed by Reddy [10] is

$$\begin{aligned} u(x, y, z) &= u_0(x, y) + f_1(z)\psi_x(x, y) + f_2(z)\frac{\partial w_0}{\partial x}, \\ v(x, y, z) &= v_0(x, y) + f_1(z)\psi_y(x, y) + f_2(z)\frac{\partial w_0}{\partial y}, \\ w(x, y, z) &= w_0(x, y), \end{aligned} \tag{2.1}$$

where

$$\begin{aligned} f_1(z) &= C_1 z - C_2 z^3, \\ f_2(z) &= -4C_4 z^3. \end{aligned} \tag{2.2}$$

Introducing $C_1 = 1$, $C_2 = C_4 = 0$, the displacement field can be reduced to first order shear deformation theory (FSDT) of [11]. For the HSDT, the values of these constants are

$$C_1 = 1, \; C_2 = C_4 = \frac{4}{3h^2}. \tag{2.3}$$

From equation (2.1) it can be seen that this form of displacement field leads to second order derivatives in the strain vector and hence C^1 continuous elements have to be used for the FEM. The difficulties associated with C^1 elements are well known. This could be circumvented by expressing the displacement field expressed by equation (2.1) in the following form:

$$\begin{aligned} u(x, y, z) &= u_0(x, y) + f_1(z)\psi_x(x, y) + f_2(z)\theta_x(x, y), \\ v(x, y, z) &= v_0(x, y) + f_1(z)\psi_y(x, y) + f_2(z)\theta_y(x, y), \\ w(x, y, z) &= w_0(x, y), \end{aligned} \tag{2.4}$$

where $\theta_x = \partial w_0/\partial x$ and $\theta_y = \partial w_0/\partial y$.

The strain vector will now contain only first order derivatives. However, the number of degrees of freedom (DOF) per node increases from 5 to 7. In this investigation, a nine noded isoparametric Lagrangian element has been used, leading to 63 DOF per element.

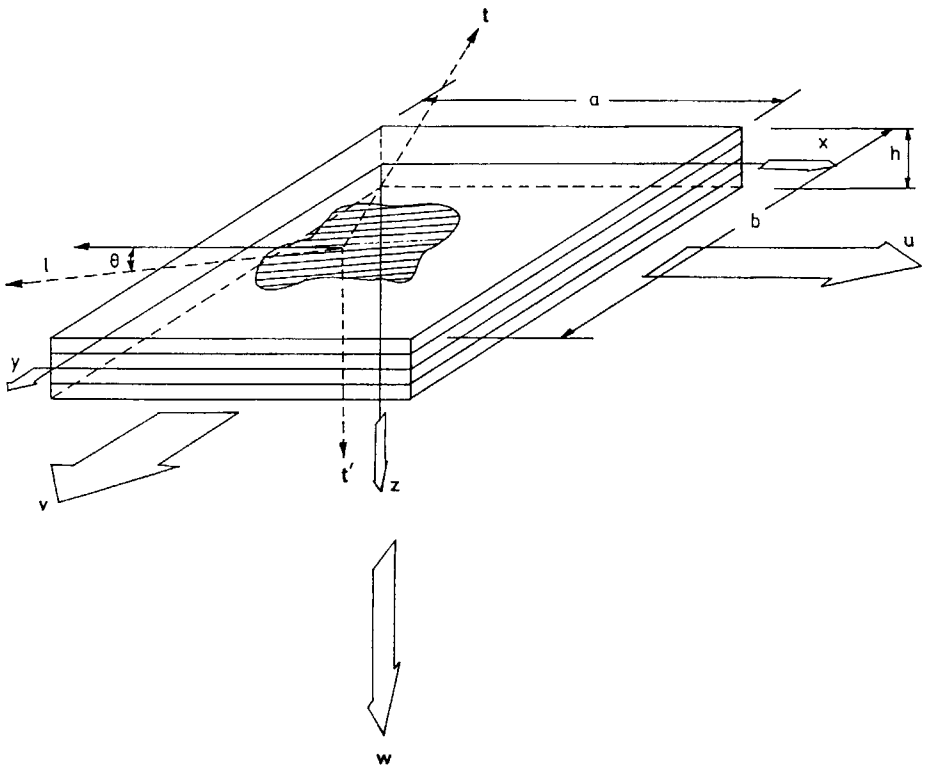

Figure 1. Laminate geometry and coordinate system.

2.2. Strain displacement relations

The strain displacement relations based on equation (2.4) following small deformation are as follows:

$$\begin{aligned}\{\varepsilon_b\} &= \{\varepsilon_x\ \varepsilon_y\ \gamma_{xy}\}^T = \{\varepsilon_1\} + z(\kappa_1) + z^3\{\kappa_2\},\\ \{\varepsilon_s\} &= \{\gamma_{yz}\ \gamma_{xz}\}^T = \{\varepsilon_2\} + z^3\{\kappa_3\},\end{aligned} \tag{2.5}$$

where $\{\varepsilon_b\}$ is the bending strain vector and $\{\varepsilon_s\}$ is the shear strain vector. Further,

$$\begin{aligned}\{\varepsilon_1\} &= \{u_{0,x}\ v_{0,y}\ u_{0,y} + v_{0,x}\}^T,\\ \{\varepsilon_2\} &= C_1\{\psi_y\ \psi_x\}^T + \{w_{0,y} + w_{0,x}\}^T,\\ \{\kappa_1\} &= C_1\{\psi_{x,x} + \psi_{y,y} - \psi_{x,y} + \psi_{y,x}\}^T,\\ \{\kappa_2\} &= -C_2\{\psi_{x,x}\ \psi_{y,y}\ \psi_{x,y} + \psi_{y,x}\}^T\\ &\quad -C_4\{\theta_{x,x}\ \theta_{y,y}\ \theta_{x,y} + \theta_{y,x}\}^T,\\ \{\kappa_3\} &= -3C_2\{\psi_y\ \psi_x\}^T - C_4\{\theta_y\ \theta_x\}^T.\end{aligned} \tag{2.6}$$

The displacement vector $\{\delta\}$ is

$$\{\delta\} = \{u_0\ v_0\ w_0\ \theta_y\ \theta_x\ \psi_y\ \psi_x\}^T. \tag{2.7}$$

The stress–strain relations for the kth lamina with respect to the reference coordinate system are

$$\begin{Bmatrix} \sigma_x \\ \sigma_y \\ \tau_{xy} \\ \tau_{yz} \\ \tau_{xz} \end{Bmatrix}_k = \begin{bmatrix} \overline{Q}_{11} & \overline{Q}_{12} & \overline{Q}_{16} & 0 & 0 \\ \overline{Q}_{12} & \overline{Q}_{22} & \overline{Q}_{26} & 0 & 0 \\ \overline{Q}_{16} & \overline{Q}_{26} & \overline{Q}_{66} & 0 & 0 \\ 0 & 0 & 0 & \overline{Q}_{44} & \overline{Q}_{45} \\ 0 & 0 & 0 & \overline{Q}_{45} & \overline{Q}_{55} \end{bmatrix}_k \begin{Bmatrix} \varepsilon_x \\ \varepsilon_y \\ \gamma_{xy} \\ \gamma_{yz} \\ \gamma_{xz} \end{Bmatrix}_k . \tag{2.8}$$

where $[\overline{Q}_{ij}]$ are the transformed stiffness coefficients for the kth lamina.

2.3. Laminate constitute equation

Instead of working with stresses which are functions of x, y and z, it is convenient to work with stress resultants, namely forces and moments per unit width. These are obtained by integrating the stresses along the thickness direction. These are defined as

$$\begin{bmatrix} N_x & M_x & P_x \\ N_y & M_y & P_y \\ N_{xy} & M_{xy} & P_{xy} \end{bmatrix} = \sum_{k=1}^{NL} \int_{z_{k-1}}^{z_k} \begin{Bmatrix} \sigma_x \\ \sigma_y \\ \sigma_{xy} \end{Bmatrix}_k (1, z, z^3)\, dz,$$

$$\begin{Bmatrix} R_y & R_y \\ Q_x & Q_x \end{Bmatrix} = \sum_{k=1}^{NL} \int_{z_{k-1}}^{z_k} \begin{Bmatrix} \tau_{yz} \\ \tau_{xz} \end{Bmatrix} (1, z^2)\, dz, \tag{2.9}$$

where NL is the number of layers in the laminate.

2.4. Finite element modeling

A nine noded isoparametric Lagrangian element has been employed for discretizing the laminate. The displacement vector $\{\delta\}$ and the geometry are represented as

$$\{\delta\} = \sum_{i=1}^{NN} N_i \{\delta_i\}, \tag{2.10}$$

$$x = \sum_{i=1}^{NN} N_i x_i, \tag{2.11}$$

$$y = \sum_{i=1}^{NN} N_i y_i, \tag{2.12}$$

where NN represents the number of nodes per element. N_i is the shape function of the ith node.

The strain vector of equation (2.6) can be expressed as

$$
\begin{aligned}
\{\varepsilon_1\} &= [L_1]\{\delta\},\\
\{\varepsilon_2\} &= [L_2]\{\delta\},\\
\{\kappa_1\} &= [L_3]\{\delta\},\\
\{\kappa_2\} &= [L_4]\{\delta\},\\
\{\kappa_3\} &= [L_5]\{\delta\}.
\end{aligned}
\tag{2.13}
$$

In equation (2.13) $[L_1], \ldots, [L_5]$ are matrices of differential operators. These are given by

$$
L_1 = \begin{bmatrix} \dfrac{\partial}{\partial x} & 0 & 0\,0\,0\,0\,0 \\ 0 & \dfrac{\partial}{\partial y} & 0\,0\,0\,0\,0 \\ \dfrac{\partial}{\partial y} & \dfrac{\partial}{\partial x} & 0\,0\,0\,0\,0 \end{bmatrix},
$$

$$
L_2 = \begin{bmatrix} 0\,0 & \dfrac{\partial}{\partial y} & 0\,0\,C_1 & 0 \\ 0\,0 & \dfrac{\partial}{\partial x} & 0\,0 & 0 & C_1 \end{bmatrix},
$$

$$
L_3 = \begin{bmatrix} 0\,0\,0\,0\,0 & 0 & C_1\dfrac{\partial}{\partial x} \\ 0\,0\,0\,0\,0\,C_1\dfrac{\partial}{\partial y} & 0 \\ 0\,0\,0\,0\,0\,C_1\dfrac{\partial}{\partial x} & C_2\dfrac{\partial}{\partial y} \end{bmatrix},
\tag{2.14}
$$

$$
L_4 = -\begin{bmatrix} 0\,0\,0 & 0 & C_4\dfrac{\partial}{\partial x} & 0 & C_2\dfrac{\partial}{\partial x} \\ 0\,0\,0\,C_4\dfrac{\partial}{\partial y} & 0 & C_2\dfrac{\partial}{\partial y} & 0 \\ 0\,0\,0\,C_4\dfrac{\partial}{\partial x} & C_4\dfrac{\partial}{\partial y} & C_2\dfrac{\partial}{\partial x} & C_2\dfrac{\partial}{\partial y} \end{bmatrix},
$$

$$
L_5 = -3\begin{bmatrix} 0\,0\,0\,C_4 & 0 & C_2 & 0 \\ 0\,0\,0 & 0 & C_4 & 0 & C_2 \end{bmatrix}.
$$

The strain displacement matrix $[B]$ for the ith node is written as

$$
[B]_i = [\mathbb{L}]N_i, \tag{2.15}
$$

where

$$[\mathbb{L}] = \begin{bmatrix} \frac{\partial}{\partial x} & 0 & 0 & 0 & 0 & 0 & 0 \\ 0 & \frac{\partial}{\partial y} & 0 & 0 & 0 & 0 & 0 \\ \frac{\partial}{\partial y} & \frac{\partial}{\partial x} & 0 & 0 & 0 & 0 & 0 \\ 0 & 0 & 0 & 0 & 0 & 0 & C_1\frac{\partial}{\partial x} \\ 0 & 0 & 0 & 0 & 0 & C_1\frac{\partial}{\partial y} & 0 \\ 0 & 0 & 0 & 0 & 0 & C_1\frac{\partial}{\partial x} & C_1\frac{\partial}{\partial y} \\ 0 & 0 & 0 & 0 & -C_4\frac{\partial}{\partial x} & 0 & -C_2\frac{\partial}{\partial x} \\ 0 & 0 & 0 & -C_4\frac{\partial}{\partial y} & 0 & -C_2\frac{\partial}{\partial y} & 0 \\ 0 & 0 & 0 & -C_4\frac{\partial}{\partial x} & -C_4\frac{\partial}{\partial y} & -C_2\frac{\partial}{\partial x} & -C_2\frac{\partial}{\partial y} \\ 0 & 0 & \frac{\partial}{\partial y} & 0 & 0 & C_1 & 0 \\ 0 & 0 & \frac{\partial}{\partial x} & 0 & 0 & 0 & C_1 \\ 0 & 0 & 0 & -3C_4 & 0 & -3C_2 & 0 \\ 0 & 0 & 0 & 0 & -3C_4 & 0 & -3C_2 \end{bmatrix}. \tag{2.16}$$

The element stiffness matrix $[K]^{(e)}$ can be expressed as

$$[K]^{(e)} = \int_{A^{(e)}} [B]^T [D][B]\,\mathrm{d}A, \tag{2.17}$$

in which $[D]$ is the material matrix, given by

$$[D] = \begin{bmatrix} [A_1] & [B] & [E] & 0 & 0 \\ [B] & [D_1] & [F_1] & 0 & 0 \\ [E] & [F_1] & [H] & 0 & 0 \\ 0 & 0 & 0 & [A_2] & [D_2] \\ 0 & 0 & 0 & [D_2] & [F_2] \end{bmatrix}. \tag{2.18}$$

The elements of plate stiffness matrices $A_{1ij}, B_{ij}, \ldots, H_{ij}$ are defined as

$$A_{1ij}, B_{ij}, D_{1ij}, E_{ij}, F_{1ij}, H_{ij} = \sum_{k=1}^{NL} \int_{z_{k-1}}^{z_k} (\overline{Q}_{ij})_k (1, z, z^2, z^3, z^4, z^6)\, \mathrm{d}z, \quad i, j = 1, 2 \text{ and } 6, \tag{2.19}$$

$$A_{2ij}, D_{2ij}, F_{2ij} = \sum_{k=1}^{NL} \int_{z_{k-1}}^{zk} (\overline{Q}_{ij})_k (1, z^2, z^4)\, \mathrm{d}z, \quad i, j = 4, 5.$$

The element stiffness matrix in terms of natural coordinate ξ, η can be written as

$$[k_{ij}] = \int_{-1}^{1} \int_{-1}^{1} [B_i]^T [D][B_j] \det[J]\, \mathrm{d}\xi \mathrm{d}\eta, \tag{2.20}$$

in which

$$[J] = \begin{bmatrix} \dfrac{\mathrm{d}x}{\mathrm{d}\xi} & \dfrac{\mathrm{d}y}{\mathrm{d}\xi} \\ \dfrac{\mathrm{d}x}{\mathrm{d}\eta} & \dfrac{\mathrm{d}y}{\mathrm{d}\eta} \end{bmatrix}. \tag{2.21}$$

2.5. Total potential of the laminate

The total potential of the laminate due to bending is given by

$$\Pi = \sum_{e=1}^{NE} \Pi^{(e)} = \sum_{e=1}^{NE} U^{(e)} + \sum_{e=1}^{NE} V^{(e)}. \tag{2.22}$$

Here, NE is the number of elements into which the total domain is discretized,

$$U^{(e)} = \frac{1}{2} \int_{A^{(e)}} \{\overline{\varepsilon}\}^T [D] \{\overline{\varepsilon}\}\, \mathrm{d}A. \tag{2.23}$$

Substituting for $\{\overline{\varepsilon}\}$ from equation (2.13) we get

$$U^{(e)} = \frac{1}{2} \int_{A^{(e)}} \left\{ \{\delta\}^T [\mathbb{L}]^T [D] [\mathbb{L}] \{\delta\} \right\} \mathrm{d}A. \tag{2.24}$$

Substituting equation (2.10) in equation (2.24) we obtain

$$U^{(e)} = \frac{1}{2} \int_{A^{(e)}} \left\{ \left(\sum_{i=1}^{NN} \{\delta_i\}^T [\mathbb{L}]^T N_i \right) [D] \left(\sum_{i=1}^{NN} [\mathbb{L}] N_i \{\delta_i\} \right) \right\} \mathrm{d}A. \tag{2.25}$$

Making use of equation (2.15), we get

$$U^{(e)} = \frac{1}{2}\int_{A^{(e)}} \left(\{d\}^T[B]^T[D][B]\{d\}\right) \mathrm{d}A, \tag{2.26}$$

where $\{d\}$ is the generalised displacement vector.

The elemental potential energy due to the external load is given by

$$V^{(e)} = -\frac{1}{2}\int_{A^{(e)}} \{\delta\}^T\{\overline{q}\}\,\mathrm{d}A, \tag{2.27}$$

where $\{\overline{q}\}$ is the load vector corresponding to each DOF.

Substitution for $\{\delta\}$ from equation (2.10) we obtain

$$\begin{aligned} V^{(e)} &= -\int_{A^{(e)}} \left(\sum_{i=1}^{NN} N_i\{\delta_i\}^T\right)\{\overline{q}_i\}^{(e)}\,\mathrm{d}A \\ &= -\{d\}^{(e)T}\{F\}^{(e)}, \end{aligned} \tag{2.28}$$

where

$$\{F\}^{(e)} = \int_{(e)} \{N\}^{(e)}\{\overline{q}\}^{(e)}\,\mathrm{d}A. \tag{2.29}$$

Minimization of the total potential with respect to $\{d\}$ leads to the equilibrium equation governing the bending of the laminate. Substituting for $U^{(e)}$ and $V^{(e)}$ from equation (2.26) and equation (2.28) in equation (2.22) and minimizing with respect to $\{d\}$, we obtain

$$[K]\{d\} + \{F\} = 0, \tag{2.30}$$

in which

$$\{d\} = \sum_{e=1}^{NE}\{d\}^{(e)},$$

$$[K] = \sum_{e=1}^{NE}[K]^{(e)},$$

$$\{F\} = -\sum_{e=1}^{NE}\{F\}^{(e)}.$$

Equation (2.30) is then solved for any given configuration and material to obtain displacements.

3. SOLUTION APPROACH — MONTE CARLO TECHNIQUE

The stiffness matrix $[K]$ involves the material properties which are treated as *RV*s. Using the second order statistics of the material properties which are treated

as independent random variables, the second order statistics of the response are obtained by using the Monte Carlo approach. In this technique a set of random numbers are generated to fit the material property mean and SD. These are used to numerically solve for the plate response values to obtain a sample of the response. The sample is analysed to evaluate the response statistics.

3.1. Input sample generation

A set of samples of random numbers are generated with available software having a given size, mean and standard deviation. The samples are checked for shift from the target mean (μ) and standard deviation (σ) which are usually present to a small extent because of numerical round-off. The shifts in the mean and the standard deviation are removed in the following manner.

3.2. Removal of shift in mean and SD

If x_i ($i = 1, 2, \ldots, n$) is a set a pseudo-random numbers, then the mean is given by

$$\mu = \sum_{i=1}^{n} \frac{x_i}{n}. \tag{3.1}$$

The sample with μ_{desired} is obtained by offsetting each of the x_i by a constant $\varepsilon = (\mu - \mu_{\text{desired}})$. The constraints for offsetting are

if $\varepsilon < 0$, the sample with μ_{desired} is increased by adding $|\varepsilon|$ to each number,
if $\varepsilon > 0$, the numbers are reduced by an amount ε.

The standard deviation, σ, of the set of random numbers can be obtained from the relations

$$\sigma^2 = \sum_{i=1}^{n} \frac{(x_i - \mu)^2}{n}. \tag{3.2}$$

Then deviation in SD,

$$\varepsilon_{\text{SD}} = \frac{\sigma_{\text{desired}}}{\sigma}. \tag{3.3}$$

Each number is multiplied by the ε_{SD} to get a scaled sample with σ_{desired} as the standard deviation. The corrections are carried out for the SD first followed by the mean.

4. SOLUTION OF GOVERNING EQUATION

The governing equation (2.30) has been solved in conjunction with the finite element technique. As stated earlier, a 7-DOF, C^0 continuity model with a 9-noded Lagrangian element is employed. The plate is discretized into the required number of elements using a mass generation module. With simple changes in the input

data, isotropic, orthotropic and anisotropic laminates can be analysed. Element stiffnesses are assembled with the help of a connectivity matrix, and boundary conditions are appropriately employed to the boundary elements. Depending on the nature of loading, the element force vector is generated and assembled. A NAG solver is used to obtain the deflection. The statistical information, like the mean and standard deviation of the deflection, is then obtained.

5. RESULTS AND DISCUSSION

Table 3 shows the convergence study carried out on a square, moderately thick plate ($a/h = 10.0$) of isotropic material, simply supported on all edges and subjected to a uniform loading $q = 100\ \mathrm{N/m^2}$. From the table it is observed that a 5×5 mesh gives very good engineering accuracy.

Table 4 shows the result for a study carried out on a 1 m square composite plate for two different loading situations. Results are compared with the values obtained by Shankara [12]. Results appear to be well within the acceptable variations.

Table 3.
Convergence study for a square isotropic plate with all edges simply supported

Mesh size	Non dimensional displacement, $\overline{w} \times 10^{-2}$
2×2	4.397522
3×3	4.616823
4×4	4.654705
5×5	5.643798

$\overline{w} = wE_t h^3/(qa^4)$; $\nu = 0.3$; $q = 100\ \mathrm{N/m^2}$; $a/h = 10.0$.

Table 4.
Validation study on a square composite laminate

Loading	a/h	θ	$\overline{w}$ (present)	FSDT [12]	HSDT [12]
Uniform	10	15°	0.9459	0.9698	0.9512
		30°	0.9157	0.9518	0.9302
		45°	0.8790	0.8919	0.8708
	100	15°	0.6962	0.7095	0.7090
		30°	0.7537	0.7690	0.7686
		45°	0.7428	0.7284	0.7281
Sinusoidal	10	15°	0.5970	0.6350	0.6218
		30°	0.5748	0.6167	0.6015
		45°	0.5501	0.5765	0.5618
	100	15°	0.4374	0.4765	0.4763
		30°	0.4680	0.4550	0.4551
		45°	0.4595	0.4694	0.4592

$\overline{w} = wE_t h^3/(qa^4)$; $E_l = 40E_t$; $G_{lt} = G_{lz} = 0.66E_t$; $G_{tz} = 0.5E_t$; $\nu_{lt} = 0.25$; $q = 100\ \mathrm{N/m^2}$.

The material properties that are considered to be random for the purposes of the study are E_l, E_t, G_{lt} and G_{tz}. Samples are generated with the standard deviation varying from 2 to 20% of their mean values with a sample size of 1000. Ten such samples are used for each study. The mean values of the properties for T300, graphite/epoxy used for computation are presented in Table 5.

In the first set of studies, dispersion of one random variable is assessed, while all other random variables are kept constant at their mean values. The geometric parameters like aspect ratio (AR), ply orientation, thickness ratio (a/h) and boundary conditions are varied. Results are computed for 4-ply anti-symmetric angle-ply laminates. The plate is uniformly loaded with intensity $q = 1000\ \mathrm{N/m^2}$. Displacements are computed at the mid point of the plate.

Figures 2 to 6 show the response of the plate for each input RVs (E_l, E_t, ν_{lt}, G_{lt} and G_{tz}), respectively. For these sets of figures, unless otherwise specified, the square laminate ($a = 1.0$ m) is simply supported on all edges with $a/h = 10$ and [45°/−45°/45°/−45°] ply orientations. Figure 2 shows the plate response for different values of normalized σ_{E_l}. For small values of σ_{E_l} the response is linear. However, it is slightly nonlinear for large values of σ_{E_l}. The dispersion in the displacement value is found to be maximum for $a/h = 100$ (thin plate). From the figure, it is observed that the dispersion in displacement is very significant in the cases of change in AR and change in thickness as compared to a change in ply orientations.

Figure 3 shows the standard deviation in displacement for different values of σ_{E_t}. Here again it is observed that thin plates are affected more than thick plates; but the changes are much less compared to when E_l is randomly varying. This observation is valid even for variation in aspect ratio, fiber orientation and boundary conditions. The plates with fiber orientation of 15° show higher sensitivity as compared to 0° laminate.

Figure 4 shows the effect of dispersion in major Poisson's ratio ν_{lt} on standard deviation of maximum displacement. It is observed that the displacement characteristics of the SS case are affected more than the plate with CC edge. Here, again thin plates are affected more than thick plates.

The effect of input random variables G_{lt} and G_{tz} on the response is shown in Fig. 5. The 0° laminate and a plate with $a/h = 100$ is affected maximum by change in G_{lt} and G_{tz}.

The response for input random variable G_{lz} is presented in Fig. 6. The response curves for both SS and CC boundary conditions almost coincide with each other.

Table 5.
Mean properties of T300/5208, graphite/epoxy composite

$E_l = 145$ GPa	$G_{lt} = 4.5$ GPa
$E_t = 10.7$ GPa	$G_{lz} = 4.5$ GPa
$\nu_{lt} = 0.31$	$G_{tz} = 3.5906$ GPa

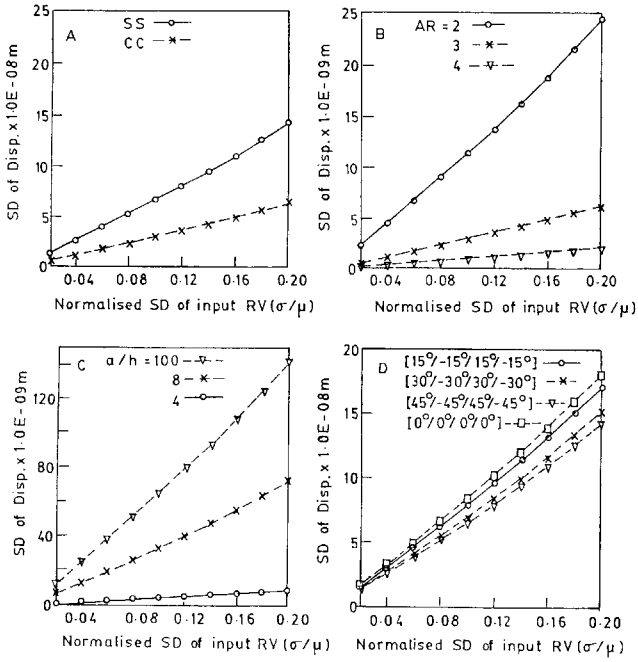

Figure 2. Deflection characteristics of laminates with σ_{E_l}.

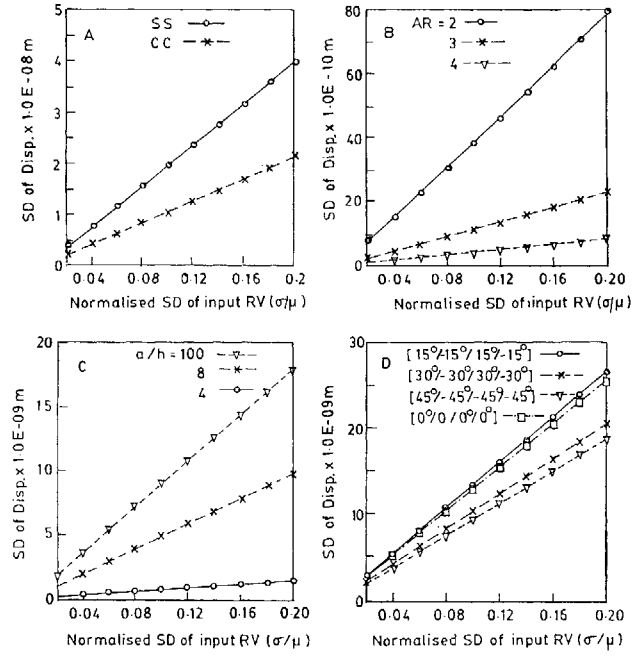

Figure 3. Deflection characteristics of laminates with σ_{E_t}.

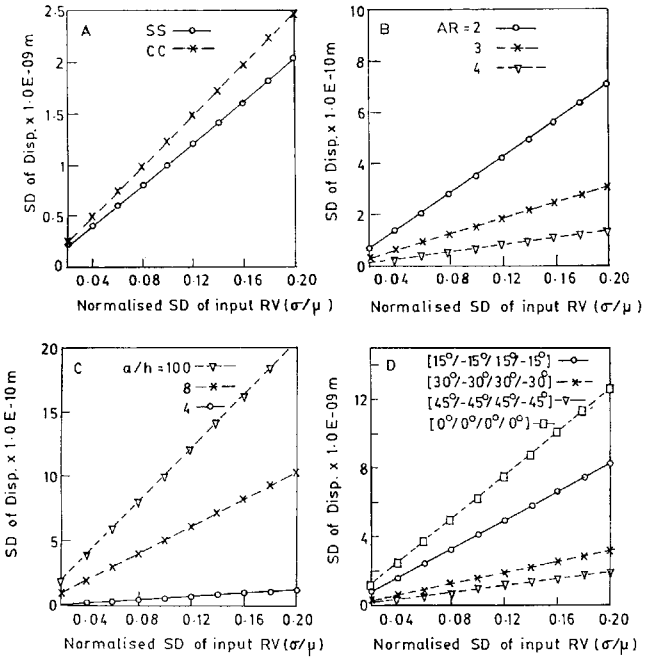

Figure 4. Deflection characteristics of laminates with $\sigma_{v_{lt}}$.

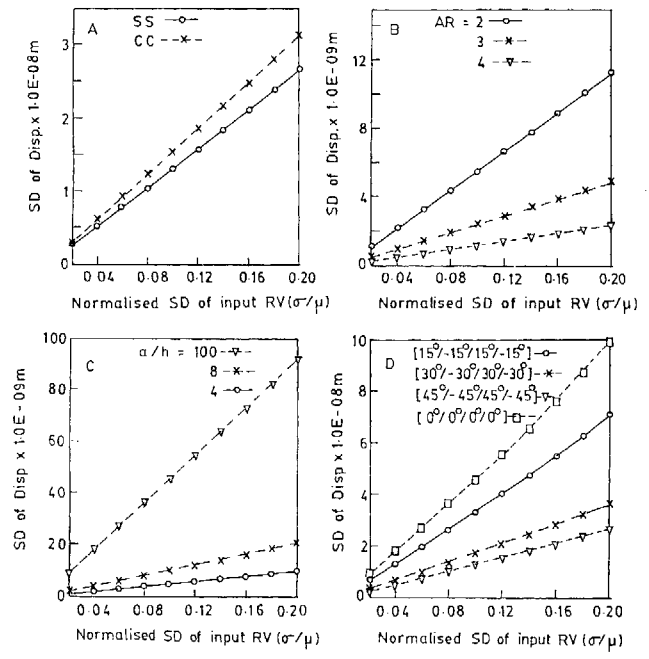

Figure 5. Deflection characteristics of laminates with $\sigma_{G_{lt}}$ and $\sigma_{G_{tz}}$.

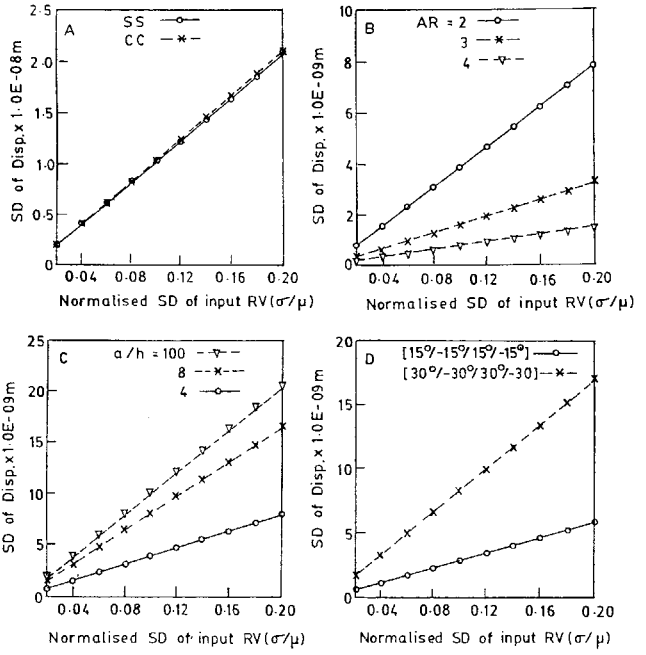

Figure 6. Deflection characteristics of laminates with $\sigma_{G_{lz}}$.

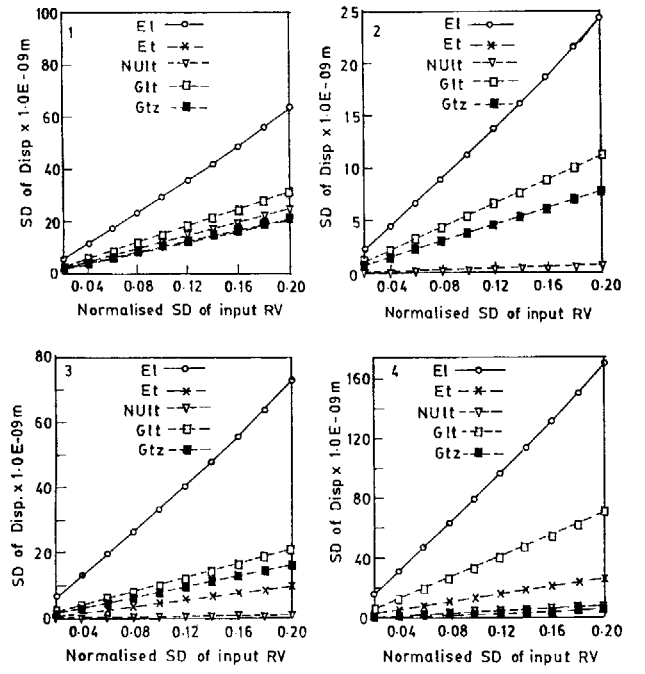

Figure 7. Response sensitivity of the laminate with material property randomness.

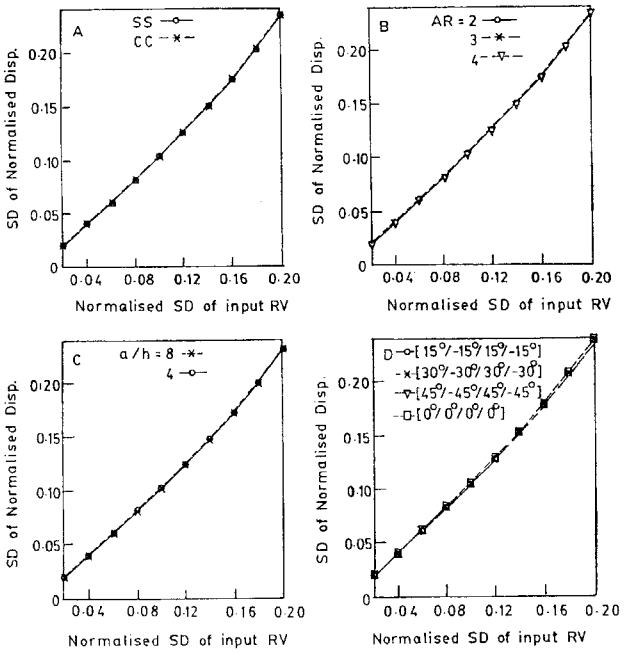

Figure 8. Normalized response characteristics of laminates.

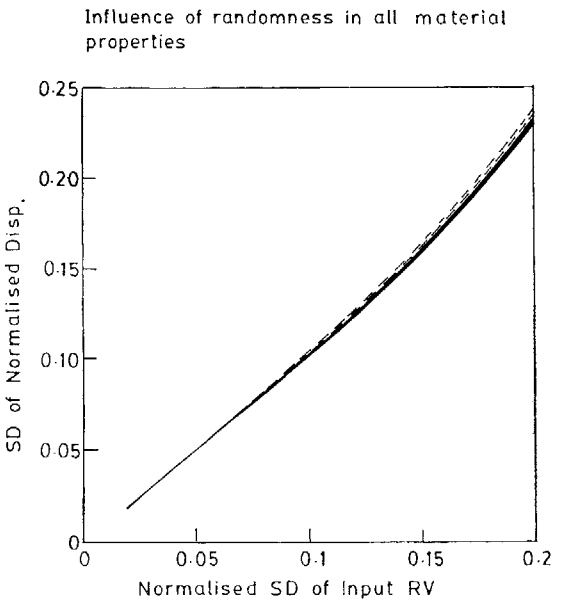

Figure 9. Plate response characteristics.

The behaviour for all other characteristics, in general, resemble the response shown in Fig. 5.

In the second set of investigations, all the material properties namely E_l, E_t, ν_{lt}, G_{lt}, G_{lz} and G_{tz} vary simultaneously, each assuming the same value for the ratio of its standard deviation to mean. The displacement SDs are presented in Fig. 7. The displacement standard deviation, normalized with the mean displacement of the laminate when all the material properties are given their mean values, is shown in Fig. 8. It is observed that the different curves for aspect ratio, boundary condition, thickness ratio and fiber orientation variation are very similar in nature. All these individual curves fall into a single curve as shown in Fig. 9 with slight dispersion in the values at higher values of input SD. The curve becomes nonlinear beyond 10% of the input variable σ. The standard deviation of normalized displacement is 25% for a 20% change in the standard deviation of input variable.

6. CONCLUSIONS

On the basis of the limited investigation carried out, the following observations can be made.

- The longitudinal modulus E_l and in-plane shear modulus G_{lt} are the most critical material properties as they considerably influence the deflection characteristics of the laminate.
- Thin plates ($a/h \geqslant 100$) are most sensitive to the variation of input material characteristics.
- The response of the laminate is linear fro small dispersion in material properties ($< 10\%$); for higher values of dispersion the response in nonlinear.
- The normalized characteristic curves of the plate with different AR, a/h, boundary conditions and ply orientation collapse into a single curve with a tolerance of 1.5% of SD of output.

Acknowledgement

Financial support received from the Structures Panel of Aeronautics Research and Development Board, Ministry of Defence, Government of India is gratefully acknowledged.

REFERENCES

1. C. Zweben, H. T. Hahn and T. W. Chow, Mechanical behaviour and properties of composite materials, in: *Delaware Composite Design Encyclopedia,* Vol. 1. Technomic, Lancaster (1989).
2. R. A. Ibrahim, Structural dynamic with parameter uncertainties, *Trans. ASME, Appl. Mech. Rev.* **40**, 309–328 (1987).
3. S. Nakagiri, H. Takabatake and S. Tani, Uncertain eigenvalue analysis of composite laminated plates by SFEM, *Compos. Struct.* **109**, 9–12 (1987).

4. A. W. Leissa and A. F. Martin, Vibration and buckling of rectangular composite plates with variable fiber spacing, *Compos. Struct.* **4**, 339–357 (1990).
5. S. P. Englestad and J. N. Reddy, Probabilistic methods for the analysis of metal matrix composites, *Compos. Sci. Technol.* **50**, 91–107 (1994).
6. G. V. Vinckenroy and W. P. de Wilde, The use of Monte-Carlo technique in SFEM for determination of the structural behaviour of composites, *Compos. Struct.* **32**, 247–253 (1995).
7. S. Salim, D. Yadav and N. G. R. Iyengar, Analysis of composite plates with random material characteristics, *Mechan. Res. Commun.* **20**, 405–414 (1993).
8. S. Salim, D. Yadav and N. G. R. Iyengar, Deflection of composite plates with random material characteristics, in: *Proc. Int. Symp. on Aerospace Science and Engineering*, Bangalore, India, pp. 236–239 (1992).
9. S. Salim, D. Yadav and N. G. R. Iyengar, Free vibration of composite plates with randomness in material properties, in: *Proc. Fifth Int. Conf. on Recent Adv. in Struct. Dyn.*, Southampton, UK, pp. 814–823 (1994).
10. J. N. Reddy, A simple higher order theory for laminated composite plates, *Trans. ASME, J. Appl. Mech.* **51**, 745–752 (1984).
11. P. C. Yang, C. H. Norris and Y. Stavsky, Elastic wave propagation in heterogeneous plates, *Int. J. Solids, Struct.* **2**, 665–684 (1966).
12. C. A. Shankara, Analysis of composite laminated plates subjected to mechanical, hygral and thermal loadings, PhD Thesis, Department of Aerospace Engineering, IIT Kanpur, pp. 43–81 (1993).